Investigation of HZETRN 2010 as a Tool for Single Event Effect Qualification of Avionics Systems

Kristina Rojdev[1] and Steve Koontz[2]
NASA Johnson Space Center, Houston, TX, 77058

William Atwell[3]
Retired Boeing Technical Fellow, Houston, TX, 77058

and

Paul Boeder[4]
Boeing Research and Technology, Houston, TX, 77058

NASA's future missions are focused on long-duration deep space missions for human exploration which offers no options for a quick emergency return to Earth. The combination of long mission duration with no quick emergency return option leads to unprecedented spacecraft system safety and reliability requirements. It is important that spacecraft avionics systems for human deep space missions are not susceptible to Single Event Effect (SEE) failures caused by space radiation (primarily the continuous galactic cosmic ray background and the occasional solar particle event) interactions with electronic components and systems. SEE effects are typically managed during the design, development, and test (DD&T) phase of spacecraft development by using heritage hardware (if possible) and through extensive component level testing, followed by system level failure analysis tasks that are both time consuming and costly. The ultimate product of the SEE DD&T program is a prediction of spacecraft avionics reliability in the flight environment produced using various nuclear reaction and transport codes in combination with the component and subsystem level radiation test data. Previous work by Koontz, et al.[1] utilized FLUKA, a Monte Carlo nuclear reaction and transport code, to calculate SEE and single event upset (SEU) rates. This code was then validated against in-flight data for a variety of spacecraft and space flight environments. However, FLUKA has a long run-time (on the order of days). CREME96[2], an easy to use deterministic code offering short run times, was also compared with FLUKA predictions and in-flight data. CREME96, though fast and easy to use, has not been updated in several years and underestimates secondary particle shower effects in spacecraft structural shielding mass. Thus, this paper will investigate the use of HZETRN 2010[3], a fast and easy to use deterministic transport code, similar to CREME96, that was developed at NASA Langley Research Center primarily for flight crew ionizing radiation dose assessments. HZETRN 2010 includes updates to address secondary particle shower effects more accurately, and might be used as another tool to verify spacecraft avionics system reliability in space flight SEE environments.

Nomenclature

AMeV	=	Mega-electron volt; unit of energy
AP8	=	integral proton flux for low Earth orbit
CERN	=	European Council for Nuclear Research

[1] Aerospace Engineer, Systems Engineering & Test Branch, 2101 NASA Parkway/MC:EA351, AIAA Member.
[2] International Space Station System Manager for Space Environments, 2101 NASA Parkway/MC:ES4, AIAA Member.
[3] Retired, 16623 Park Green Way, AIAA Associate Fellow.
[4] Aerospace Engineer, Space Environments, 13100 Space Center Blvd./HB3-20, non-member.

CREME = Cosmic Ray Effects on Microelectronics
DD&T = Design, Development, and Test
EPCARD = European Program package for the Calculation of Aviation Route Doses
FLUKA = FLUktuierende KAskade
FORTRAN = FORmula TRANslating System
g/cm^2 = areal density; measure of thickness in radiation calculations
GCR = Galactic Cosmic Ray
GEANT = GEometry ANd Tracking
GEO = Geostationary orbit
HUP = a CREME96 program module that evaluates direct-ionization induced SEEs
HZETRN = High-Charge and Energy Transport
INFN = Italian National Institute for Nuclear Physics
ITAR = International Traffic in Arms Regulations
km = kilometers
LEO = Low Earth Orbit
LET = Linear Energy Transfer
SEE = Single Event Effect
SEU = Single Event Upset
SPE = Solar Particle Event
SPENVIS = SPace ENVironment Information System
TID = Total Ionizing Dose

I. Introduction

THE character of long-term (1-3 years) human interplanetary space flight will lead to safety and reliability requirements more demanding (and costly) than any previously encountered. To date, spacecraft crews have never been more than a few hours-to-days away from a safe emergency landing. There are no comparable quick/safe Earth return options for the crew of an interplanetary transport a few months out from Earth. In that case, spacecraft systems failures really aren't an option. Avionics systems reliability depends on generic hardware/software quality as well as component/system sensitivity to the space radiation environment, especially the total ionizing dose (TID) and single event effects (SEE) environments.

Spacecraft are designed and built to meet specific safety and reliability requirements and the production of data products demonstrating that the spacecraft will meet those requirements is a standard part of the spacecraft design development and test (DD&T) phase of the project. Spacecraft avionics systems SEE test and verification processes have been previously described[4-7] and have most often involved ground based testing of avionics components with the test results feeding into a system level reliability and safety analysis using the expected mission SEE environment.

Calculation of the expected spacecraft avionics system in-flight SEE environments using a nuclear reaction and transport code is an important step in the avionics system SEE reliability analysis[8]. The nuclear reaction and transport code calculates the environment resulting from the interaction of the natural space radiation charged particle environment with the spacecraft shielding mass and reports back both primary and secondary charged particle fluxes expected at the avionics system along with any secondary low LET protons or neutrons that can also contribute to SEE effects. The SEE environment is described primarily by the Linear Energy Transfer (LET) spectrum. LET is a measure of how much ionization/excitation an energetic charged particle produces on passing through matter, and space radiation effects on avionics are determined by charged particle LET. SEE caused by very low LET protons or neutrons also depend on the LET of charged nuclear reaction products formed inside microelectronic devices when the neutrons or protons collide with nuclei inside the device.

Spacecraft SEE environments calculated with nuclear reaction and transport codes play an important role in both human and robotic interplanetary flight programs so that the precision, accuracy, and ease of use of such codes are important considerations for any flight program. Monte Carlo codes, like FLUKA, accurately capture verified nuclear and particle physics and produce high accuracy results, but require massive computational resources and can need execution times on the order of days to weeks for even very simple spacecraft geometries. Deterministic codes, like CREME96 and HZETRN can execute quickly on personal computers, enabling configuration comparison studies on complex 3D spacecraft geometries, but may not have the desired precision and accuracy. Often the Monte Carlo codes are used to benchmark and support development of more accurate deterministic codes, as previously described[9-11].

HZETRN[12] was developed primarily to support human space flight radiological health requirements. LET and secondary neutron spectra are basic to calculating effective or equivalent space radiation dose to astronauts. HZETRN 2010 is a recent update to the HZETRN family and includes a more accurate representation of secondary particle shower products. In the following, LET spectra calculations produced with CREME96 and HZETRN 2010 are compared at different aluminum shielding mass thicknesses for both the interplanetary GCR environment and the International Space Station low-Earth orbit environment. Finally, space flight SEU rates are compared with rate predictions made using both deterministic codes.

II. Background

A. CREME96

CREME96[2] is based on the earlier work[13-16] by Dr. Jim Adams, formerly of the Naval Research Laboratory, Washington, DC, and University of Alabama, Huntsville. The Cosmic Ray Effects on Microelectronics (CREME) software package allows a spacecraft designer or operator to estimate error rates arising from cosmic ray bombardment of satellite microelectronics. Program functions include calculation of (1) differential and integral cosmic ray flux (for any element) vs. particle energy or vs. linear energy transfer (LET), (2) geomagnetic shielding for a given orbit using the tabulation of geomagnetic cutoff values by Shea and Smart[17] as described by Ref. 14, (3) ordinary and worst-case solar flare proton fluxes, and (4) single event upset rates for microelectronics in the orbiting satellite.

B. HZETRN

The high-charge-and-energy (HZE) transport (TRN) computer program, HZETRN[12], was developed at NASA Langley Research Center to address the problems of space radiation transport and shielding. The HZETRN[18] program is intended specifically for the design engineer who is interested in obtaining fast and accurate dosimetric information for the design and construction of space modules and devices. The program is based on a one-dimensional space-marching formulation of the Boltzmann transport equation with a straight-ahead approximation. The effect of the long-range Coulomb force and electron interaction is treated as a continuous slowing-down process. Atomic (electronic) stopping power coefficients with energies above a few AMeV are calculated by using Bethe's theory including Bragg's rule, Ziegler's shell corrections, and effective charge. Nuclear absorption cross sections are obtained from fits to quantum calculations and total cross sections are obtained with a Ramsauer formalism. Nuclear fragmentation cross sections are calculated with a semi-empirical abrasion-ablation fragmentation model. The relation of the final computer code to the Boltzmann equation is discussed in the context of simplifying assumptions.

The HZETRN code is a state-of-the-art fast computational tool available for a design engineer to obtain answers to some of the radiation questions that arise in planning any mission. However, major uncertainties in nuclear cross sections, environmental models, and astronaut risk affect the overall accuracy of the predictions of any analytical-computational technique. These uncertainties have a major impact on the proposed shield design for any mission and the subsequent mission cost. Much work remains to accurately resolve the problems with nuclear cross-section calculations, environmental model development, and risk estimate methods. The most recent release of the HZETRN code is HZETRN 2010 and can be obtained from Dr. Martha Clowdsley, although the code is ITAR-controlled.

III. Methods

To generate the HZETRN data, two input spectra were used and were the same as those in Ref. 1 to keep consistent. The first one was a low Earth orbit (LEO) environment that was at an altitude of 362.5 km and an inclination of 51.6°. This was from the AP8 solar minimum model of May 2006 (Figure 1). This spectrum was generated using SPENVIS and then interpolated against the HZETRN 2010 energy grid.

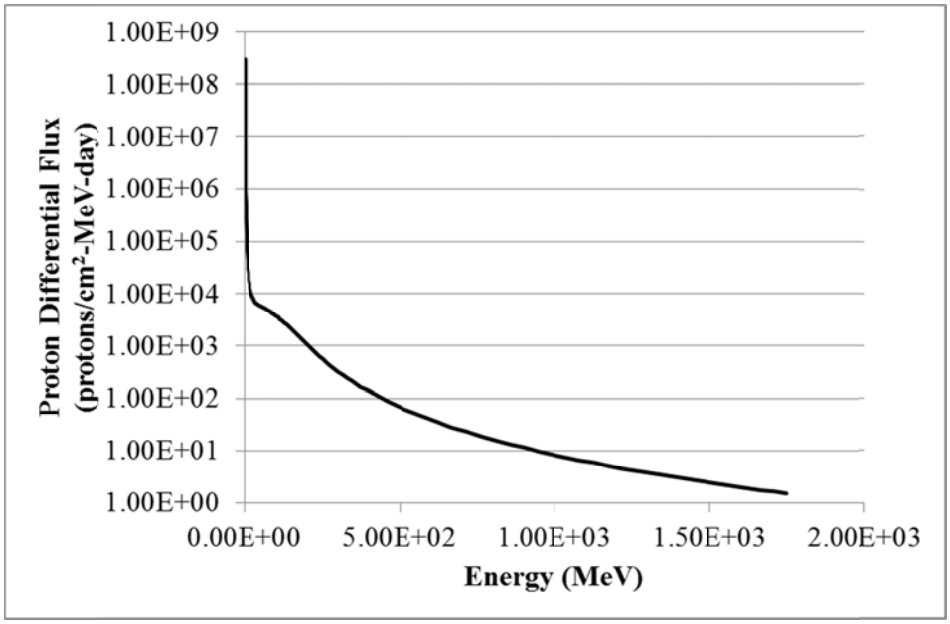

Figure 1. AP8 May 2006 solar minimum differential flux.

The second was the 1977 solar minimum free space GCR environment (Figure 2). Solar minimum leads to higher intensity GCR exposure due to the inverse relationship between solar activity and GCR activity. This spectrum was part of the pre-coded environments within HZETRN 2010. For CREME96, the same SPE and GCR environments were used but they were the environments available in CREME96.

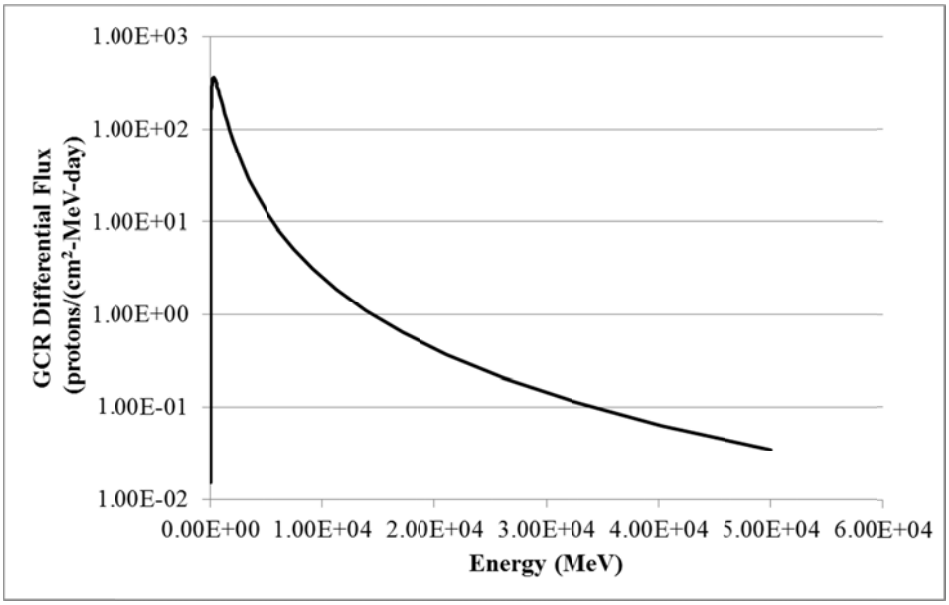

Figure 2. 1977 solar minimum GCR differential flux.

For the runs in HZETRN 2010, an aluminum shield profile was used to simulate a spacecraft. The thicknesses used in the profile were the following: 0.0, 0.1, 0.5, 1.0, 5.0, 10.0, 20.0, 50.0, 100.0, 150.0, and 200.0 g/cm^2. Since we are concerned with electronics in this study, a silicon detector was used. For the runs in CREME96, the same shielding profile was used as in HZETRN 2010, but only to 50 g/cm^2 because the CREME96 code can only generate spectra for thicknesses out to this range. Therefore the data shown below will only encompass the thicknesses out to 50 g/cm^2.

The outputs from HZETRN 2010 were differential and integral LET spectra at each thickness. These LET spectra were then compared with the spectra from CREME96. Further analysis was then completed with CREME96 using the LET spectra from both codes to generate SEE rates.

IV. Results

A subset of the integral flux LET spectra generated from HZETRN 2010 and CREME96 are compared in Figure 3-Figure 5 for the LEO orbit and Figure 6-Figure 8 for the GCR environment. The remaining data for the LEO integral flux can be found in Appendix A and the remaining data for the GCR integral flux can be found in Appendix B.

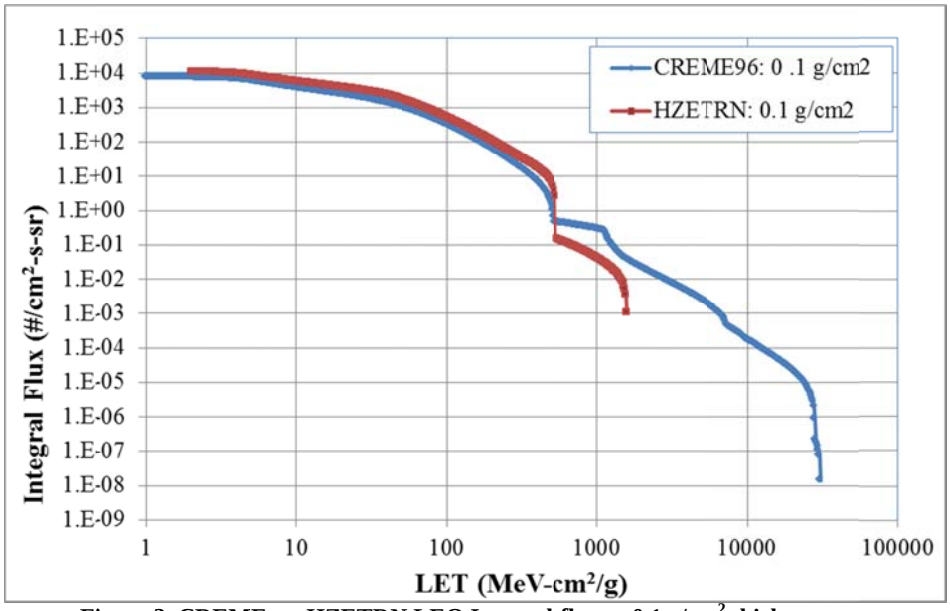

Figure 3. CREME vs. HZETRN LEO Integral flux at 0.1 g/cm^2 thickness.

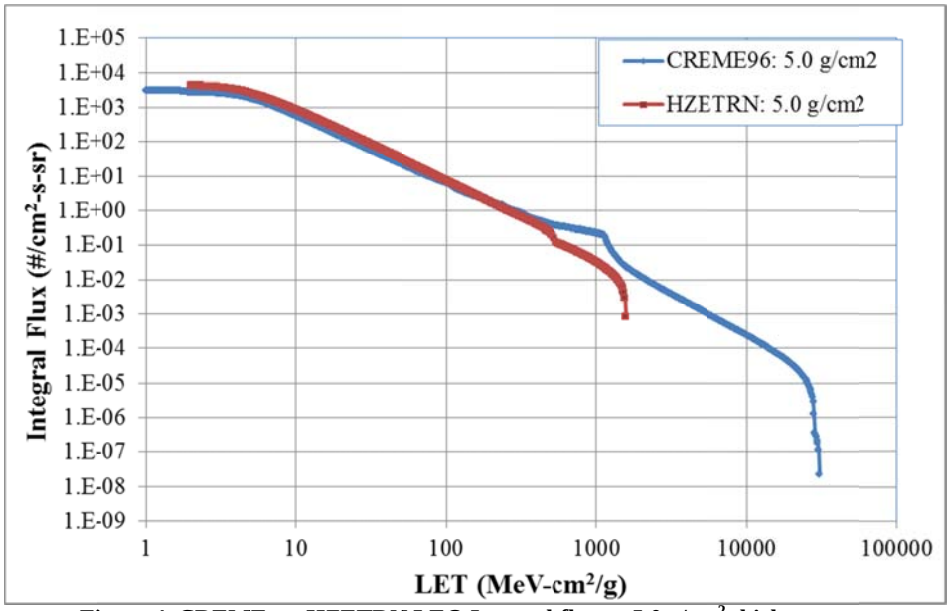

Figure 4. CREME vs. HZETRN LEO Integral flux at 5.0 g/cm^2 thickness.

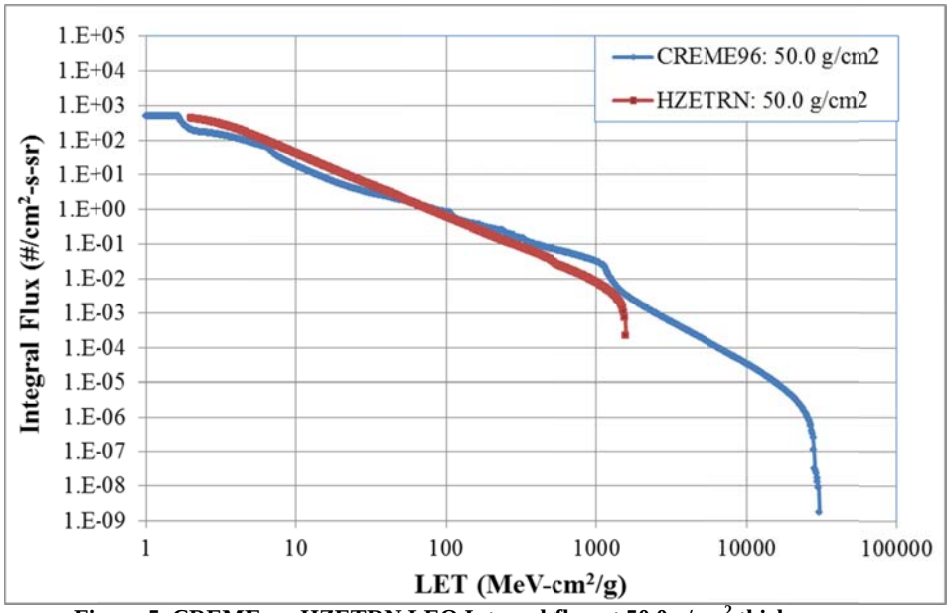

Figure 5. CREME vs. HZETRN LEO Integral flux at 50.0 g/cm^2 thickness.

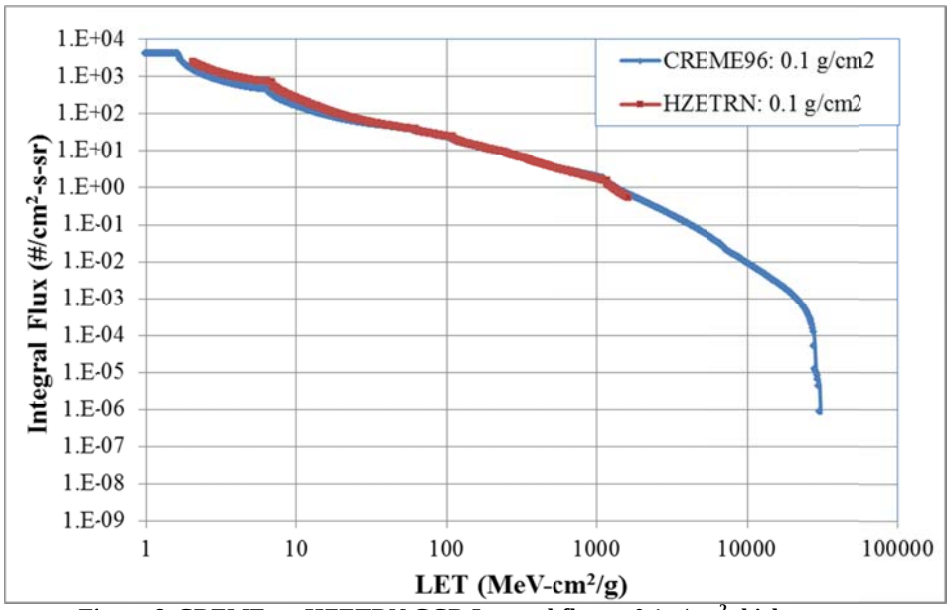

Figure 6. CREME vs. HZETRN GCR Integral flux at 0.1 g/cm^2 thickness.

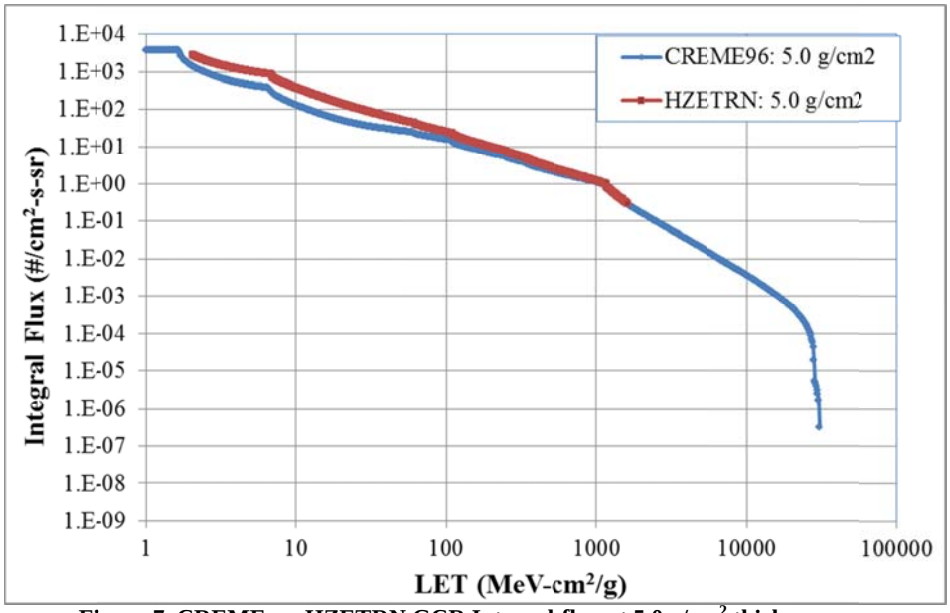

Figure 7. CREME vs. HZETRN GCR Integral flux at 5.0 g/cm^2 thickness.

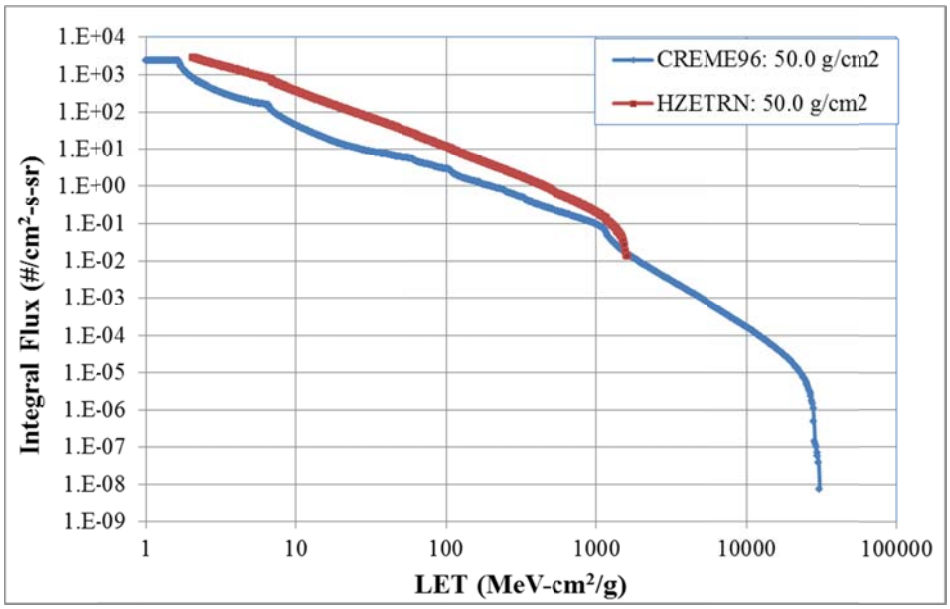

Figure 8. CREME vs. HZETRN GCR Integral flux at 50.0 g/cm2 thickness.

The current version of HZETRN 2010 only includes elements out to Nickel (Z = 28), so CREME96 spectra were similarly constrained to a maximum of Z = 28. HZETRN 2010 also only outputs a maximum LET of 1,566 MeV-cm^2/g for the LEO environment and 11,692 MeV-cm^2/g for the GCR environment as compared to 30,364 MeV-cm^2/g for CREME96 (for max Z = 28). The impact of these limitations in the HZETRN 2010 spectra on SEE rate calculations will now be investigated.

Radiation characterization parameters for several devices flown either on ISS, GEO, or deep space missions are given in Table 1[1]. The table shows SEE sensitive volume dimensions and Weibull fit parameters for each device.

Table 1. Device Parameters.

Device	Env	CREME96 RPP x,y,z (μm)	Onset (MeV- cm^2/mg)	Width (MeV- cm^2/mg)	Exponent	Limiting XS (μm^2)
IMS1601EPI	ISS	39.5, 39.5, 5.92	2.75	140	0.95	1560
ISS SMJ416400 4Mx4 DRAM	ISS	1.05, 1.05, 2.1	0.42	0.8	1.7	1.1
ISS KM44S32030T 128Mbit SDRAM	ISS	2.42, 2.42, 0.24	13	30	1	5.859
ISS KM44S32030T 128Mbit SDRAM	ISS	1.25, 1.25, 0.125	14	30	1	1.563
ISS KM44S32030T 128Mbit SDRAM	ISS	0.43, 0.43, 0.043	1.95	30	1.9	0.186
V4 XQR4VFX60 – BRAM	ISS	1.87, 1.87, 3.74	0.2	70	0.724	3.5
V4 XQR4VFX60 – Config. Memory	ISS	5.1, 5.1, 10.2	0.5	400	0.985	26
V5 LX330T – Config. Memory	ISS	3.36, 3.36, 6.72	0.5	30	1.5	11.3
Thuraya DSP Mega gate ASIC	GEO	2.5, 2.5, 1.76	2.7	20.6	1.2	6.3
Mercury Messenger ASIC	GEO	2, 2, 2	0.3	60	6	4
Cassini OKI Solid State Recorder	GEO	6.32, 6.32, 6.32	0.5	32	3	40
SOHO SMJ44100 4Mx1	GEO	7.07, 7.07, 2	0.7	15	2.7	50
SOHO MHS CP65656EV 32kx8 SRAM	GEO	7.75, 7.75, 2	1.9	17	1.2	60
ETS-V PD4464D-20 64k SRAM	GEO	19, 19, 10	0.5	15	2.9	375

SEE rates were calculated for these devices for four different LET spectra variations using the CREME96 HUP heavy ion SEE rate calculator. The four different LET spectra variations are showing in the following table.

Table 2. LET Spectra Variations

Code	Max Z	Max GEO LET (MeV-cm^2/g)	Max LEO LET (MeV-cm^2/g)	Min LET (MeV-cm^2/g)
HZETRN	28	11596	1578	1
CREME96 (Z=28 truncated)	28	11596	1578	1
CREME96	28	30364	30364	1
CREME96	92	101000	101000	1

To calculate SEE rates with CREME96 HUP using the HZETRN 2010 LET spectra, the spectra were first modified to conform to the CREME96 LET spectra limits and interval spacing. They were then imported into the CREME96 website. The CREME96 (Z=28 Truncated) spectra were generated in a similar fashion by truncating the standard CREME96, max Z = 28 output LET spectra and importing it back into the CREME96 website. SEE rates for a subset of the LET spectra variations are given in Table 3-Table 5 for LEO environment devices and Table 6-Table 8 for GEO and free space environment devices. The remaining tables for the other shielding configurations can be found in Appendix A for the LEO environment and Appendix B for the GEO and free space environments. All shielding depths are aluminum equivalent. Note that for the 50 g/cm^2 thickness (Table 5 and Table 8) there is no data for CREME96 (Z=92) due to the inability of CREME96 to handle thicknesses around 50 g/cm^2 or larger.

Table 3. SEE Rate for LEO Devices at 0.1 g/cm^2

Depth = 0.1 g/cm^2	SEE/bit-day			
LEO Environment Devices	**HZETRN Z=28**	**CREME96 Z=28 Truncated**	**CREME96 Z=28**	**CREME96 Z=92**
IMS1601EPI	1.84E-06	1.37E-06	1.76E-06	1.77E-06
ISS SMJ416400 4Mx4 DRAM	4.49E-08	1.08E-07	1.31E-07	1.31E-07
ISS KM44S32030T 128Mbit SDRAM	4.19E-11	2.37E-10	1.33E-09	1.34E-09
ISS KM44S32030T 128Mbit SDRAM	5.92E-12	3.38E-11	2.97E-10	2.98E-10
ISS KM44S32030T 128Mbit SDRAM	5.11E-10	3.25E-10	4.09E-10	4.10E-10
V4 XQR4VFX60 – BRAM	9.62E-07	4.62E-07	4.61E-07	4.67E-07
V4 XQR4VFX60 – Config. Memory	2.54E-09	8.11E-09	1.10E-08	1.10E-08
V5 LX330T – Config. Memory	9.99E-10	4.56E-09	8.82E-09	8.85E-09

Table 4. SEE Rate for LEO Devices at 5.0 g/cm^2

Depth = 5.0 g/cm^2	SEE/bit-day			
LEO Environment Devices	**HZETRN Z=28**	**CREME96 Z=28 Truncated**	**CREME96 Z=28**	**CREME96 Z=92**
IMS1601EPI	1.65E-07	6.87E-07	9.24E-07	9.27E-07
ISS SMJ416400 4Mx4 DRAM	1.46E-08	7.72E-08	9.02E-08	9.04E-08
ISS KM44S32030T 128Mbit SDRAM	3.20E-11	1.64E-10	8.73E-10	8.79E-10
ISS KM44S32030T 128Mbit SDRAM	4.52E-12	2.27E-11	1.94E-10	1.95E-10
ISS KM44S32030T 128Mbit SDRAM	2.79E-11	1.05E-10	1.55E-10	1.55E-10
V4 XQR4VFX60 – BRAM	2.69E-08	6.05E-08	6.30E-08	6.33E-08
V4 XQR4VFX60 – Config. Memory	1.11E-09	6.03E-09	7.67E-09	7.70E-09
V5 LX330T – Config. Memory	6.11E-10	3.40E-09	5.99E-09	6.01E-09

Table 5. SEE Rate for LEO Devices at 50.0 g/cm2

Depth = 50.0 g/cm^2	SEE/bit-day		
LEO Environment Devices	**HZETRN Z=28**	**CREME96 Z=28 Truncated**	**CREME96 Z=28**
IMS1601EPI	3.50E-08	1.05E-07	1.39E-07
ISS SMJ416400 4Mx4 DRAM	3.40E-09	1.12E-08	1.30E-08
ISS KM44S32030T 128Mbit SDRAM	8.08E-12	2.17E-11	1.22E-10
ISS KM44S32030T 128Mbit SDRAM	1.15E-12	3.03E-12	2.73E-11
ISS KM44S32030T 128Mbit SDRAM	5.53E-12	1.60E-11	2.31E-11
V4 XQR4VFX60 – BRAM	4.30E-09	1.01E-08	1.05E-08
V4 XQR4VFX60 – Config. Memory	2.62E-10	8.70E-10	1.10E-09
V5 LX330T – Config. Memory	1.46E-10	4.80E-10	8.49E-10

Table 6. SEE Rate for GEO Devices at 0.1 g/cm^2

Depth = 0.1 g/cm^2	SEE/bit-day			
GEO Environment Devices	**HZETRN Z=28**	**CREME96 Z=28 Truncated**	**CREME96 Z=28**	**CREME96 Z=92**
Thuraya DSP Mega gate ASIC	7.74E-08	1.08E-07	1.13E-07	1.13E-07
Mercury Messenger ASIC	1.92E-12	2.54E-12	3.56E-11	3.65E-11
Cassini OKI Solid Sta te Recorder	2.82E-08	3.81E-08	5.96E-08	5.99E-08
SOHO SMJ44100 4Mx1	1.11E-06	1.45E-06	1.49E-06	1.49E-06
SOHO MHS CP65656EV 32kx8 SRAM	2.91E-06	3.54E-06	3.58E-06	3.58E-06
ETS-V PD4464D-20 64k SRAM	5.05E-06	6.76E-06	7.15E-06	7.16E-06

Table 7. SEE Rate for GEO Devices at 5.0 g/cm^2

Depth = 5.0 g/cm^2	SEE/bit-day			
GEO Environment Devices	**HZETRN Z=28**	**CREME96 Z=28 Truncated**	**CREME96 Z=28**	**CREME96 Z=92**
Thuraya DSP Mega gate ASIC	3.70E-08	3.71E-08	3.93E-08	3.94E-08
Mercury Messenger ASIC	8.55E-13	9.93E-13	1.40E-11	1.43E-11
Cassini OKI Solid Sta te Recorder	1.33E-08	1.40E-08	2.26E-08	2.27E-08
SOHO SMJ44100 4Mx1	5.87E-07	5.65E-07	5.82E-07	5.83E-07
SOHO MHS CP65656EV 32kx8 SRAM	1.69E-06	1.56E-06	1.58E-06	1.58E-06
ETS-V PD4464D-20 64k SRAM	2.52E-06	2.51E-06	2.67E-06	2.67E-06

Table 8. SEE Rate for GEO Devices at 50.0 g/cm^2

Depth = 50.0 g/cm^2	SEE/bit-day		
GEO Environment Devices	**HZETRN Z=28**	**CREME96 Z=28 Truncated**	**CREME96 Z=28**
Thuraya DSP Mega gate ASIC	1.53E-09	1.86E-09	1.94E-09
Mercury Messenger ASIC	3.01E-14	4.54E-14	5.15E-13
Cassini OKI Solid Sta te Recorder	6.37E-10	6.97E-10	1.04E-09
SOHO SMJ44100 4Mx1	4.90E-08	3.33E-08	3.40E-08
SOHO MHS CP65656EV 32kx8 SRAM	1.97E-07	1.06E-07	1.06E-07
ETS-V PD4464D-20 64k SRAM	1.59E-07	1.36E-07	1.42E-07

Table 9 compares SEE rates calculated using the HZETRN 2010 LET spectra and CREME96 HUP with in-flight SEE rate observations.

Table 9. Flight SEE Rates Compared to HZETRN Based SEE Rates.

Device	Env	Median Shielding Mass g/cm^2	In-Flight SEU/bit day	HZETRN Predicted SEU/bit day
IMS1601EPI (1)	ISS	34	3.10E-07	<7.27E-08
ISS SMJ416400 4Mx4 DRAM	ISS	10	3.20E-09	1.06E-08
ISS SMJ416400 4Mx4 DRAM (1)	ISS	40	3.70E-09	<6.75E-09
ISS KM44S32030T 128Mbit SDRAM	ISS	40	3.30E-10	<1.18E-11
V4 XQR4VFX60 – BRAM (2)	ISS	0.8	4.20E-08	5.42E-08
V4 XQR4VFX60 – Config. Memory (2)	ISS	0.8	3.80E-09	1.62E-09
V5 LX330T – Config. Memory (2)	ISS	0.8	7.60E-09	8.81E-10
Thuraya DSP Mega gate ASIC (2)	GEO	0.7	5.30E-08	6.61E-08
Cassini OKI Solid Sta te Recorder (2)	GEO	3.4	5.80E-08	<2.40E-08
SOHO SMJ44100 4Mx1	GEO	1	5.90E-07	9.71E-07
SOHO MHS CP65656EV 32kx8 SRAM	GEO	1	1.70E-07	2.60E-06
ETS-V PD4464D-20 64k SRAM	GEO	5.8	1.70E-06	2.52E-06

Table Notes:
1) closest shielding value for HZETRN calculation is 20 g/cm^2
2) closest shielding value for HZETRN calculation is 1 g/cm^2
3) closest shielding value for HZETRN calculation is 5 g/cm^2
Median shielding mass and in-flight SEU rates taken from ref. 1.

In flight SEU rates are compared with rates calculated using HZETRN 2010 , FLUKA and CREME96 in Figure 9 below and using the accompanying least squares performance metric equations. The FLUKA and CREME96 calculations (taken from Ref. 1) are for a GCR environment with maximum Z=28 and the full LET range, while in the HZETRN 2010 calculation the LET spectrum is truncated just above 1000 MeV-cm^2/g as shown in Figure 3-Figure 8 above. The overall performance of the HZETRN 2010 calculation method is comparable to both the full-LET-range FLUKA and CREME96 methods with respect to agreement between predicted SEU rates and in-flight measurements of SEU rates. The agreement between the in-flight SEU rates and the predicted rates is acceptable for practical applications given that agreement within a "factor-of-a-few" is considered excellent in general[5] and agreement within an order of magnitude is more typical[19].

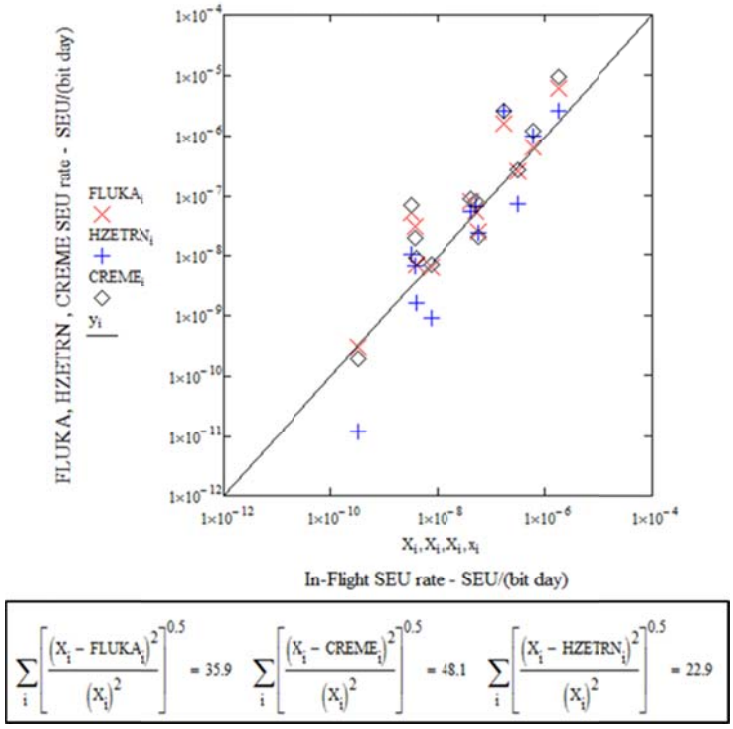

Figure 9. Comparing FLUKA, CREME, and HZETRN 2010 SEU rate estimates with in-flight SEU rates.

V. Discussion

Direct comparison of the LET spectra produced by CREME96 and HZETRN 2010 (Figure 3-Figure 8) immediately reveals an important limitation of HZETRN 2010 as applied to spacecraft avionics SEE work. The range of LET values output by the current version of HZETRN 2010 is too limited for general spacecraft SEE avionics work. Despite the limitation in LET range, cutting off just above 1000 MeV-cm^2/g, agreement with CREME96 LET spectra is reasonable in the overlapping regions for the most part. HZETRN 2010 also predicts higher fluxes at higher shielding masses, indicating a more accurate treatment of secondary particle showers than CREME96. An important exception is the LEO environment at LET values near 1000 MeV-cm^2/g, where CREME96 particle fluxes are higher than those predicted by HZETRN 2010 (Figure 3-Figure 5).

The most direct "Apples to Apples" comparison of calculated SEU rates is between the HZETRN2010 and CREME96 (GCR with maximum Z=28 and Truncated LET range) cases in Table 6-Table 8. For most of these cases, the CREME96 rates are somewhat higher, but not in all cases.

Comparison of the HZETRN 2010 based rates with CREME96 un-truncated LET spectra cases (GCR with maximum Z = 28 and GCR with maximum Z = 92) shows that the truncated HZETRN 2010 LET spectra produces significantly lower rates in most cases (Table 6-Table 8) indicating the need to extend the HZETRN 2010 LET range in order to make the code more accurate and complete for spacecraft avionics SEE work.

Comparison of the CREME96 GCR with maximum Z=28 runs with the GCR with maximum Z=92 SEE rates (Table 6-Table 8) shows that inclusion of the higher Z GCR elements had little impact on the overall SEE rates of the devices, as expected, given the very low flux of GCR particles with Z > 28. Note also that all of these devices have low or moderately low LET thresholds. Incorporating the high Z component of the environment is not so important for devices like these. The high Z elements become important for devices with higher LET thresholds and it is especially important to devices that may be susceptible to high-threshold destructive failures, such as single event latch-up and/or burn-out.

As shown in Table 9 and the accompanying regression plot and least squares figures of merit above (Figure 9), the HZETRN 2010 predictions present a mixed bag, with some device predictions exceeding observations and a few coming in significantly under the observations. The significant under-predictions are most likely a result of the truncated HZETRN 2010 LET spectra combined with higher device thresholds. Nonetheless, the performance of HZETRN 2010 in predicting in-flight SEU rates is comparable to FLUKA and CREME96 for the devices studied here.

HZETRN 2010 is a promising possible tool for spacecraft avionics SEE work in that secondary particle shower products appear to be represented more accurately in HZETRN 2010 than in CREME96, at least over the limited LET range currently available in HZETRN 2010. To make HZETRN 2010 effective for spacecraft avionics SEE rate calculations, the code would need to be updated so as to extend the LET tables out to 100,000 MeV-cm^2/g if possible.

VI. Conclusion

HZETRN 2010 shows considerable promise as a spacecraft avionics SEE analysis and qualification tool, even with the present limited LET output range. To make HZETRN 2010 fully acceptable for spacecraft avionics SEE rate calculations, the range of the LET output tables needs to be extended to between 10,000 and 100,000 MeV-cm^2/g. Future work will build upon this paper once the LET range has been extended. We will also investigate HZETRN 2010 against additional in-space flight data of more recent devices to provide further validation.

Appendix

A. LEO Data

The following graphs show additional comparisons of the integral flux LET spectra from CREME96 and HZETRN 2010 for the LEO environment.

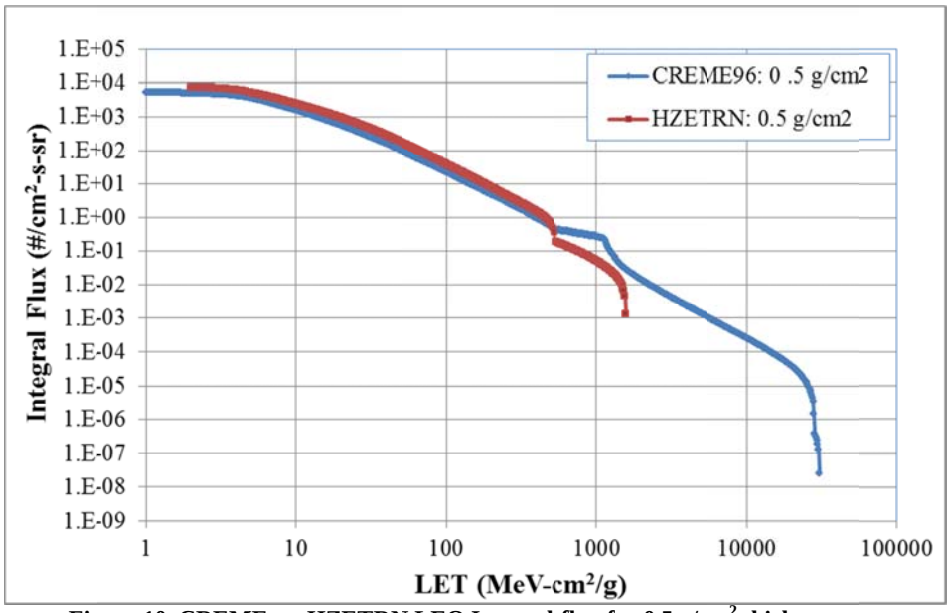

Figure 10. CREME vs. HZETRN LEO Integral flux for 0.5 g/cm^2 thickness.

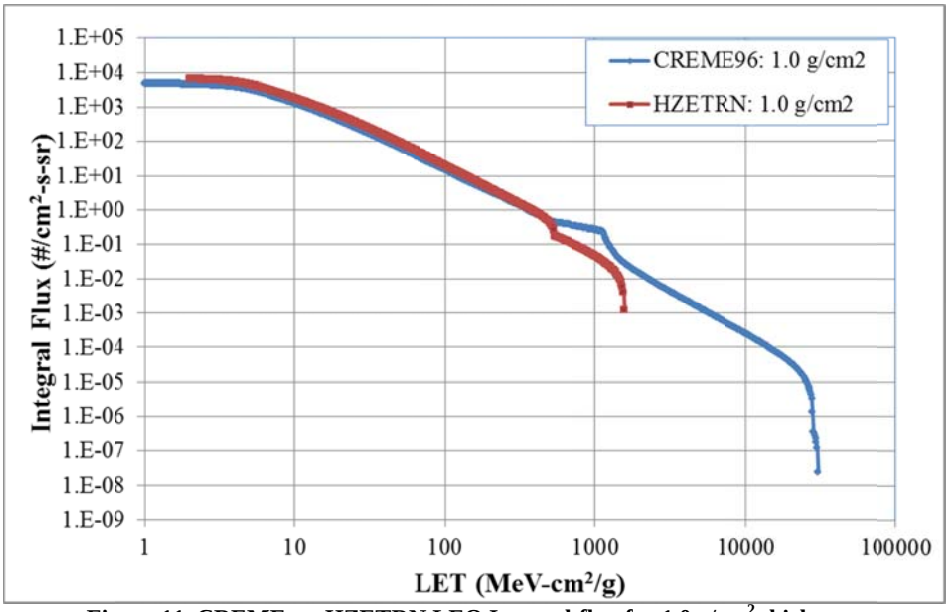

Figure 11. CREME vs. HZETRN LEO Integral flux for 1.0 g/cm^2 thickness.

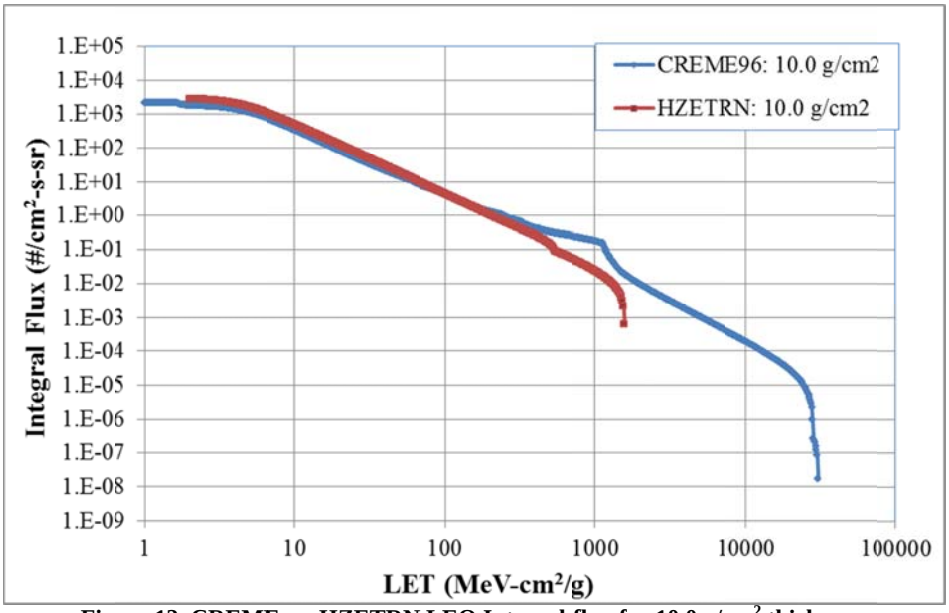

Figure 12. CREME vs. HZETRN LEO Integral flux for 10.0 g/cm^2 thickness.

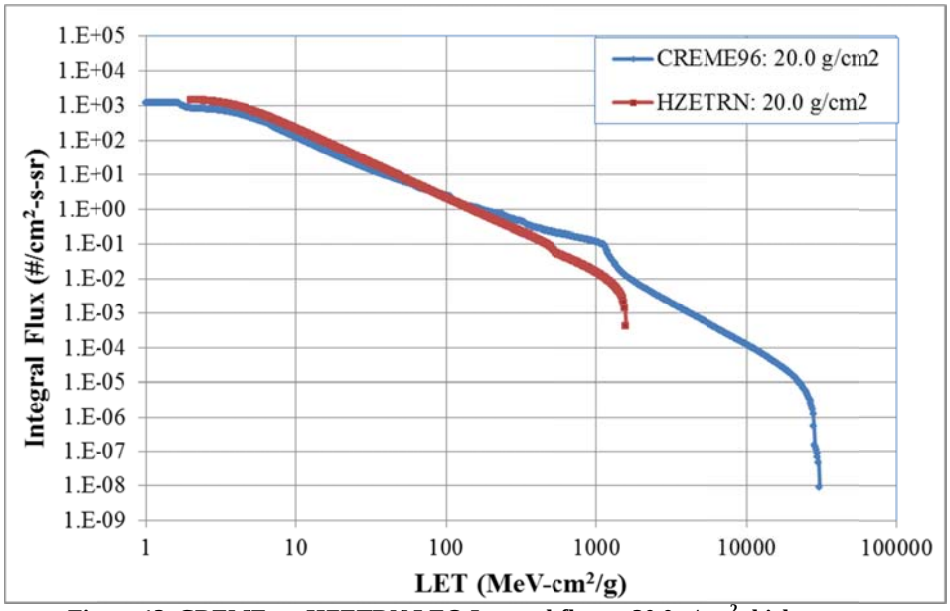

Figure 13. CREME vs. HZETRN LEO Integral flux at 20.0 g/cm^2 thickness.

The following are additional tables of SEE rates for the LET spectra variations in the LEO environment.

Table 10. SEE Rate for LEO Devices at 0.5 g/cm^2

Depth = 0.5 g/cm^2	SEE/bit-day			
LEO Environment Devices	**HZETRN Z=28**	**CREME96 Z=28 Truncated**	**CREME96 Z=28**	**CREME96 Z=92**
IMS1601EPI	3.40E-07	8.46E-07	1.11E-06	1.12E-06
ISS SMJ416400 4Mx4 DRAM	2.44E-08	9.34E-08	1.08E-07	1.09E-07
ISS KM44S32030T 128Mbit SDRAM	5.09E-11	2.00E-10	9.82E-10	9.89E-10
ISS KM44S32030T 128Mbit SDRAM	7.18E-12	2.76E-11	2.17E-10	2.18E-10
ISS KM44S32030T 128Mbit SDRAM	6.70E-11	1.34E-10	1.90E-10	1.91E-10
V4 XQR4VFX60 – BRAM	8.71E-08	8.90E-08	9.17E-08	9.23E-08
V4 XQR4VFX60 – Config. Memory	1.82E-09	7.28E-09	9.14E-09	9.18E-09
V5 LX330T – Config. Memory	9.82E-10	4.11E-09	7.00E-09	7.03E-09

Table 11. SEE Rate for LEO Devices at 1.0 g/cm^2

Depth = 1.0 g/cm^2	SEE/bit-day			
LEO Environment Devices	**HZETRN Z=28**	**CREME96 Z=28 Truncated**	**CREME96 Z=28**	**CREME96 Z=92**
IMS1601EPI	2.65E-07	8.22E-07	1.09E-06	1.09E-06
ISS SMJ416400 4Mx4 DRAM	2.14E-08	9.17E-08	1.07E-07	1.07E-07
ISS KM44S32030T 128Mbit SDRAM	4.59E-11	1.96E-10	9.73E-10	9.80E-10
ISS KM44S32030T 128Mbit SDRAM	6.48E-12	2.71E-11	2.15E-10	2.16E-10
ISS KM44S32030T 128Mbit SDRAM	4.80E-11	1.28E-10	1.83E-10	1.84E-10
V4 XQR4VFX60 – BRAM	5.42E-08	7.92E-08	8.20E-08	8.24E-08
V4 XQR4VFX60 – Config. Memory	1.62E-09	7.16E-09	9.01E-09	9.04E-09
V5 LX330T – Config. Memory	8.81E-10	4.04E-09	6.91E-09	6.95E-09

Table 12. SEE Rate for LEO Devices at 10.0 g/cm^2

Depth = 10.0 g/cm^2	SEE/bit-day			
LEO Environment Devices	**HZETRN Z=28**	**CREME96 Z=28 Truncated**	**CREME96 Z=28**	**CREME96 Z=92**
IMS1601EPI	1.18E-07	5.55E-07	7.44E-07	7.46E-07
ISS SMJ416400 4Mx4 DRAM	1.06E-08	6.21E-08	7.24E-08	7.26E-08
ISS KM44S32030T 128Mbit SDRAM	2.36E-11	1.30E-10	6.93E-10	6.97E-10
ISS KM44S32030T 128Mbit SDRAM	3.34E-12	1.80E-11	1.54E-10	1.55E-10
ISS KM44S32030T 128Mbit SDRAM	1.95E-11	8.44E-11	1.24E-10	1.25E-10
V4 XQR4VFX60 – BRAM	1.80E-08	4.88E-08	5.08E-08	5.11E-08
V4 XQR4VFX60 – Config. Memory	8.13E-10	4.85E-09	6.15E-09	6.17E-09
V5 LX330T – Config. Memory	4.48E-10	2.72E-09	4.78E-09	4.80E-09

Table 13. SEE Rate for LEO Devices at 20.0 g/cm^2

Depth = 20.0 g/cm^2	SEE/bit-day			
LEO Environment Devices	**HZETRN Z=28**	**CREME96 Z=28 Truncated**	**CREME96 Z=28**	**CREME96 Z=92**
IMS1601EPI	7.27E-08	3.65E-07	4.84E-07	4.86E-07
ISS SMJ416400 4Mx4 DRAM	6.75E-09	4.03E-08	4.69E-08	4.70E-08
ISS KM44S32030T 128Mbit SDRAM	1.53E-11	8.25E-11	4.40E-10	4.42E-10
ISS KM44S32030T 128Mbit SDRAM	2.17E-12	1.14E-11	9.77E-11	9.83E-11
ISS KM44S32030T 128Mbit SDRAM	1.18E-11	5.53E-11	8.05E-11	8.07E-11
V4 XQR4VFX60 – BRAM	1.03E-08	3.24E-08	3.37E-08	3.38E-08
V4 XQR4VFX60 – Config. Memory	5.17E-10	3.14E-09	3.97E-09	3.99E-09
V5 LX330T – Config. Memory	2.86E-10	1.76E-09	3.06E-09	3.08E-09

B. GCR Data

The following graphs show additional comparisons of the integral flux LET spectra from CREME96 and HZETRN 2010 for the GCR environment.

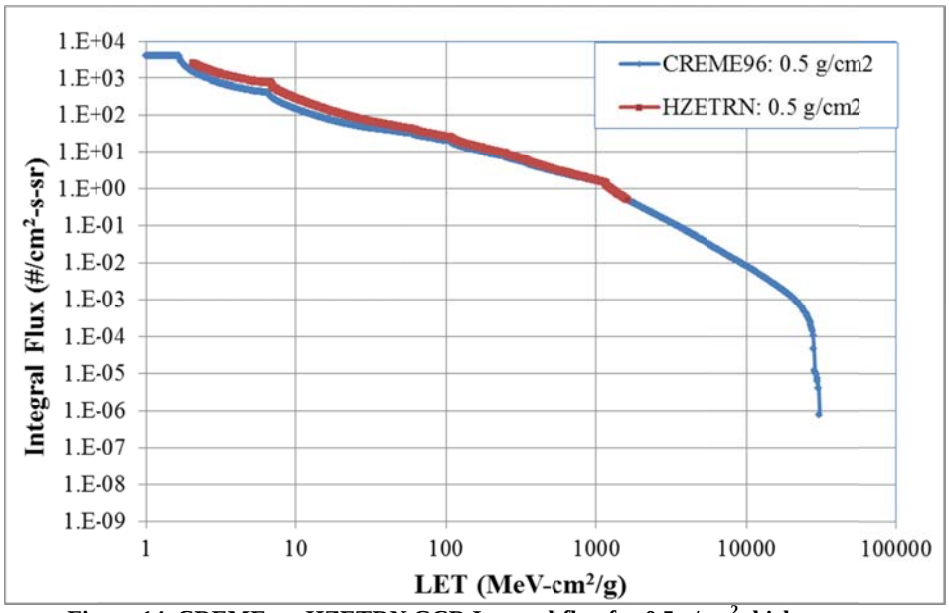

Figure 14. CREME vs. HZETRN GCR Integral flux for 0.5 g/cm^2 thickness.

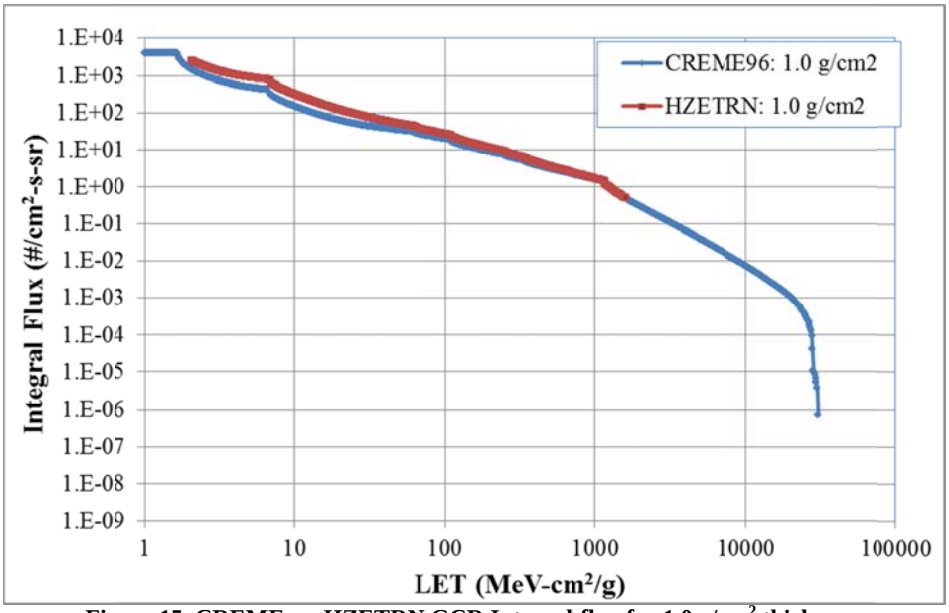

Figure 15. CREME vs. HZETRN GCR Integral flux for 1.0 g/cm^2 thickness.

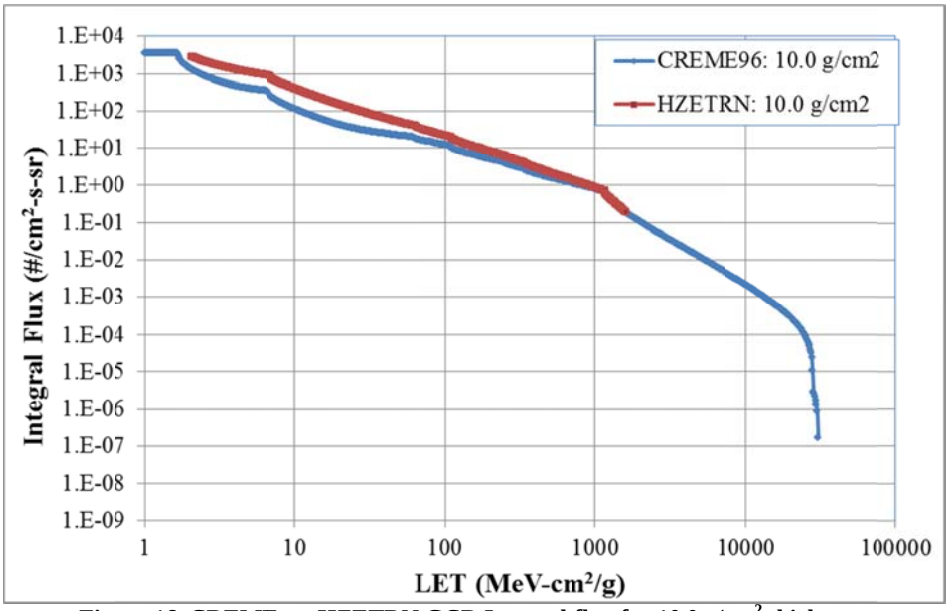

Figure 16. CREME vs. HZETRN GCR Integral flux for 10.0 g/cm^2 thickness.

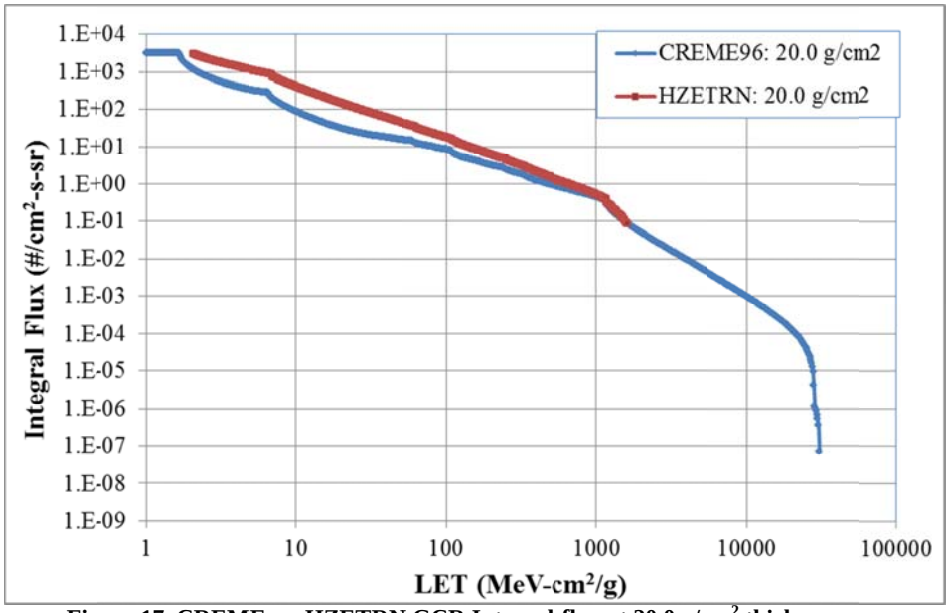

Figure 17. CREME vs. HZETRN GCR Integral flux at 20.0 g/cm^2 thickness.

The following are additional tables of SEE rates for the LET spectra variations in GEO and the free space environment.

Table 14. SEE Rate for GEO Devices at 0.5 g/cm^2

Depth = 0.5 g/cm^2	SEE/bit-day			
GEO Environment Devices	**HZETRN Z=28**	**CREME96 Z=28 Truncated**	**CREME96 Z=28**	**CREME96 Z=92**
Thuraya DSP Mega gate ASIC	7.30E-08	7.82E-08	8.33E-08	8.36E-08
Mercury Messenger ASIC	1.82E-12	2.25E-12	3.34E-11	3.42E-11
Cassini OKI Solid Sta te Recorder	2.67E-08	2.99E-08	5.02E-08	5.04E-08
SOHO SMJ44100 4Mx1	1.06E-06	1.09E-06	1.13E-06	1.13E-06
SOHO MHS CP65656EV 32kx8 SRAM	2.79E-06	2.75E-06	2.78E-06	2.79E-06
ETS-V PD4464D-20 64k SRAM	4.79E-06	5.12E-06	5.48E-06	5.49E-06

Table 15. SEE Rate for GEO Devices at 1.0 g/cm^2

Depth = 1.0 g/cm^2	SEE/bit-day			
GEO Environment Devices	**HZETRN Z=28**	**CREME96 Z=28 Truncated**	**CREME96 Z=28**	**CREME96 Z=92**
Thuraya DSP Mega gate ASIC	6.61E-08	7.08E-08	7.53E-08	7.55E-08
Mercury Messenger ASIC	1.62E-12	2.01E-12	2.97E-11	3.04E-11
Cassini OKI Solid Sta te Recorder	2.40E-08	2.70E-08	4.51E-08	4.53E-08
SOHO SMJ44100 4Mx1	9.71E-07	9.99E-07	1.03E-06	1.04E-06
SOHO MHS CP65656EV 32kx8 SRAM	2.60E-06	2.55E-06	2.58E-06	2.59E-06
ETS-V PD4464D-20 64k SRAM	4.35E-06	4.65E-06	4.97E-06	4.99E-06

Table 16. SEE Rate for GEO Devices at 10.0 g/cm^2

Depth = 10.0 g/cm^2	SEE/bit-day			
GEO Environment Devices	**HZETRN Z=28**	**CREME96 Z=28 Truncated**	**CREME96 Z=28**	**CREME96 Z=92**
Thuraya DSP Mega gate ASIC	2.22E-08	2.24E-08	2.37E-08	2.38E-08
Mercury Messenger ASIC	5.00E-13	5.87E-13	8.04E-12	8.20E-12
Cassini OKI Solid Sta te Recorder	8.04E-09	8.44E-09	1.35E-08	1.35E-08
SOHO SMJ44100 4Mx1	3.75E-07	3.58E-07	3.68E-07	3.68E-07
SOHO MHS CP65656EV 32kx8 SRAM	1.13E-06	1.03E-06	1.04E-06	1.04E-06
ETS-V PD4464D-20 64k SRAM	1.56E-06	1.55E-06	1.64E-06	1.65E-06

Table 17. SEE Rate for GEO Devices at 20.0 g/cm^2

Depth = 20.0 g/cm^2	SEE/bit-day			
GEO Environment Devices	**HZETRN Z=28**	**CREME96 Z=28 Truncated**	**CREME96 Z=28**	**CREME96 Z=92**
Thuraya DSP Mega gate ASIC	9.99E-09	1.06E-08	1.12E-08	1.12E-08
Mercury Messenger ASIC	2.16E-13	2.72E-13	3.54E-12	3.60E-12
Cassini OKI Solid Sta te Recorder	3.65E-09	3.99E-09	6.24E-09	6.26E-09
SOHO SMJ44100 4Mx1	1.88E-07	1.77E-07	1.82E-07	1.82E-07
SOHO MHS CP65656EV 32kx8 SRAM	6.09E-07	5.33E-07	5.37E-07	5.38E-07
ETS-V PD4464D-20 64k SRAM	7.41E-07	7.50E-07	7.91E-07	7.93E-07

References

[1]Koontz, S., Reddell, B., and Boeder, P., "Calculating Spacecraft Single Event Environment with FLUKA," *Radiation Effects Data Workshop*, Las Vegas, 2011.

[2]Tylka, A.J., Adams, Jr., J.H., Boberg, P.R., Brownstein, B.,Dietrich, W.F., Flueckiger, E.O., Petersen, E.L., Shea, M.A., Smart, D.F., and Smith, E.C., "CREME96: A Revision of the Cosmic Ray Effects on Micro-Electronics Code," *IEEE Trans. Nucl. Sci.* Vol. 44, 1997, pp. 2150-2160.

[3]Clowdsley, M., and Badavi, F. F., "HZETRN 2010," *private communication*, 2010.

[4]Reed, R.A., Kinnison, J., Pickel, J.C., Buchner, S., Marshall, P.W., Kniffin, S., LaBel, K.A., "Single Event Effects Ground Testing and On-orbit Rate Prediction Methods: The Past, present and Future," *IEEE Transactions on Nuclear Science*, Vol. 50 No. 3, 2003, pp. 622-634.

[5]Edmonds, L.D., Barnes, C.E., Scheick, L.Z., "An Introduction to Space Radiation Effects on Microelectronics," *JPL Publication 00-06*, Jet Propulsion Laboratory, Pasadena California, 2000.

[6]Artola, L., Velazco, R., Hubert, G., Duzellier, S., Nuns, T., Guerard, B., Peronnard, P., Mansour, W., Pancher, F., Bezerra, F., "In Flight SEU/MCU Sensitivity of Commercial Nanometric SRAMs: Operational Estimations," *IEEE Transactions on Nuclear Science*, Vol. 58, No. 6, 2011, pp. 2644- 2651.

[7]Schwank, J.R., Shaneyfelt, M.R., and Dodd, P.E., "Radiation Hardness Assurance Testing of Microelectronic Devices and Integrated Circuits: Radiation Environments, Physical Mechanisms, and Foundations for Hardness Assurance," *IEEE Transactions on Nuclear Science*, Vol. 60, No. 3, 2013, pp. 2074-2100.

[8] Reed, R.A., Weller, R.A., Akkerman, A., Barak, J., Culpepper, W., Duzellier, S., Foster, C., Gaillardin, M., Hubert, G., Jordan, T., Jun, I., Koontz, S., Lei, F., McNulty, P., Mendenhall, M.H., Murat, M., Nieminen, P., O'Neill, P., Raine, M., Reddell, B., Saigne, F., Santin, G., Sihver, L., Tang, H.H.K., Truscott, P.R., Wrobel, F., "Anthology of the Development of Radiation Transport Tools as Applied to Single Event Effects," *IEEE Transactions on Nuclear Science*, Vol. 60 , No. 3, 2013, pp. 1876 - 1911.

[9]Lin, Z., Adams, J. J., Barghouty, A., Randeniya, S., Tripathi, R., Watts, J., and Yepes, P., "Comparisons of Several Transport Models in their Predictions in Typical Space Radiation Environments," *Advances in Space Research*, Vol. 49, 2012, pp. 797-806.

[10]Heinbockel, J. H., Slaba, T. C., Blattnig, S. R., Tripathi, R. K., Townsend, L. W., Handler, T., Gabriel, T. A., Pinsky, L. S., Reddell, B., Clowdsley, M. S., Singleterry, R. C., Norbury, J. W., and Badavi, F. F., "Comparison of the transport codes HZETRN, HETC and FLUKA for a solar particle event," *Advances in Space Research*, Vol. 47, No. 6, 2011, pp. 1079-1088.

[11]Heinbockel, J. H., Slaba, T. C., Tripathi, R. K., Blattnig, S. R., Norbury, J. W., Badavi, F. F., Townsend, L. W., Handler, T., Gabriel, T. A., Pinksy, L. S., Reddell, B. and Aumann, A. R., "Comparison of the transport codes HZETRN, HETC and FLUKA for galactic cosmic rays," *Advances in Space Research*, Vol. 47, No. 6, 2011, pp. 1089-1105.

[12]Wilson, J.W., Badavi, F.F., Cucinotta, F.A., Shinn, J.L., Badhwar, G.D., Silberberg, R., Tsao, C.H., Townsend, L.W., and Tripathi, R.K., "HZETRN: Description of a Free-Space Ion and Nucleon Transport and Shielding Computer Program," *NASA Technical Paper 3495*, 1995.

[13]Adams, J. H., Silberberg, R., and Tsao, C. H., Cosmic Ray Effects on Microelectronics, Part I: The Near-Earth Particle Environment, *NRL Memorandum Report 4506 (AD-A103897)*, Navy Research Laboratory, Washington, D.C., 1981.

[14]Adams, J. H., Letaw, J. R., and Smart, D. F., "Cosmic Ray Effects on Microelectronics, Part II: The Geomagnetic Cutoff Effects," *NRL Memorandum Report 5099 (AD-A128601)*, Navy Research Laboratory, Washington, D.C., 1983.

[15]Tsao, H., Silberberg, R., Adams, J. H., and Letaw, J. R., "Cosmic Ray Effects on Microelectronics, Part III: Propagation of Cosmic Rays in the Atmosphere," *NRL Memorandum Report 5402 (AD-A145026)*, Navy Research Laboratory, Washington, D.C., 1984.

[16]Adams, J. H., "Cosmic Ray Effects on Microelectronics, Part IV," *NRL Memorandum Report 5901*, Washington, D.C., 1986.

[17]Shea, M. E. and Smart, D. F., "Tables of Asymptotic Directions and Vertical Cutoff Rigidities for a Five Degree by Fifteen Degree World Grid as Calculated Using the International Geomagnetic Reference Field for Epoch 1975.0," *Report AFCRL-TR-75-0185 (AD-A012509)*, Air Force Geophysics Laboratory, Hanscom AFB, Massachusetts, 1975.

[18]Wilson, J. W., Badavi, F. F., Cucinotta, F. A., Shinn, J. L., Badhwar, G. D., Silberberg, R., Tsao, C. H., Townsend, L. W., and Tripathi, R. K., "HZETRN: description of a Free-Space Ion and Nucleon Transport and Shielding Computer Program," *NASA TP-3495*, 1995.

[19]Petersen. E., L., "Predictions and Observations of SEU Rates in Space," *IEEE Transactions on Nuclear Science*, Vol. 44, No.6, 1997, pp. 2174-2287.